Evolutionary Systematics. 9 2025, 77–86 | DOI 10.3897/evolsyst.9.147291

PENSOFT

EVOLUTIONARY SYSTEMATICS

Protosiphonorhinus patrickmuelleri gen. et sp. nov., the first fossil member of the sucking millipede family Siphonorhinidae (Colobognatha, Siphonophorida) described from Cretaceous Myanmar amber

Leif Moritz[1], Benjamin Wipfler[1], Thomas Wesener[1]

1 *Zoological Research Museum A. Koenig (ZFMK), Leibniz Institute for the Study of Biodiversity Change (LIB), Adenauerallee 160, D-53113 Bonn, Germany*

https://zoobank.org/7BADD00C-9649-4B92-8172-8B04FD873385

Corresponding author: Thomas Wesener (t.wesener@leibniz-lib.de)

Academic editor: Stephanie F. Loria ♦ **Received** 20 January 2025 ♦ **Accepted** 2 March 2025 ♦ **Published** 17 March 2025

Abstract

Millipedes (Diplopoda) are an abundant group of fossilized terrestrial arthropods throughout the Palaeozoic Era. However, there is a gap in the Mesozoic Period with only slightly more than a dozen fossils known, until more recent fossil records – mainly from Cenozoic Dominican and Baltic ambers – became available. Here, we describe a millipede of the family Siphonorhinidae from Myanmar amber, a species-poor group, comprising just six extant genera, disjunctly distributed in Southeast Asia, South Africa, Madagascar, Chile and California. Micro-computed tomography (μ-CT) enabled detailed visualizations of essential elements for description, including the tergites, legs, head, antenna, and notably the gonopods. The new genus shares some characteristics with species of the extant genus *Siphonorhinus* Pocock, 1894. *Protosiphonorhinus patrickmuelleri* **gen. et sp. nov.** differs from extant species of the family mainly in the shape of the antenna, tergites, and anterior gonopods. A recently described fossil species of Siphonophorida from Myanmar amber was erroneously assigned to the family Siphonorhinidae. We transfer it to the family Siphonophoridae, as *Siphonophora globosa* (Su, Cai & Huang, 2024) **comb. nov**. The description of the new genus and the reinterpretation of the previously described fossil Siphonorhinidae allows for a rejection of a hypothesis of bradytely within the Siphonorhinidae from the mid-Cretaceous to the present day.

Key Words

Amber, Burmese amber, Mesozoic, Soil arthropods, Micro CT, Millipede

Introduction

Myanmar amber from the Hukawng Valley of northern Myanmar has been dated to the Upper Cretaceous Period (98 ± 0.63 Ma, Shi et al. 2012). The Cretaceous is a significant period for the evolution of terrestrial life, marked by a radiation of insects and flowering plants (Grimaldi 1999; Friis et al. 2006). Myanmar amber was the first scientifically studied Cretaceous amber and is by far the one with the highest diversity of known preserved taxa (Ross, 2018; 2022). Myanmar amber inclusions offer a window into the diversity, ecology, and evolution of this important period (Grimaldi 2002; Cruickshank and Ko 2003).

Millipedes (Diplopoda) are considered one of the first fully terrestrialized organisms and include more than 12,000 described extant species (Enghoff et al. 2015) with a high level of ecological and morphological diversity (Marek et al. 2012; Moritz et al. 2021; Su et al. 2021). As detritivores and soil-forming organisms, millipedes play an essential role in terrestrial ecosystems (Schaefer 1990; Crawford 1992; Curry 1994; Wolters and Ekschmitt 1997).

Fossils are indispensable for reconstructing the evolutionary history of millipedes, but only a few individuals have been recorded from the Mesozoic, leaving a significant gap in our knowledge (Wesener and Moritz 2018; Jiang et al. 2019; Moritz and Wesener 2021). The majority of these fossils are recorded from Myanmar amber deposits (Su et al. 2022). The millipede fauna in Myanmar amber is considered rich and represents an important diversity of species, most still undescribed (Moritz and Wesener 2018; Jiang et al. 2019). The few described species have been placed in extant orders, and the oldest known and first fossils of many millipede taxa were found in Myanmar amber, including Siphonophorida (Wesener and Moritz 2018; Jiang et al. 2019).

The Siphonophorida is one of the less-known millipede orders with rare fossil records and a currently small number of extant species reported. Around 120 of the 12,000 extant millipede species are Siphonophorida, representing only about 1% of known millipede species diversity (Jeekel 2001; Read and Enghoff 2018). This group is often referred to as a "taxonomist's nightmare" due mainly to its lack of well-defined characters for description (Hoffman 1980; Jeekel 2001; Moritz and Parra-Gómez 2023).

Siphonophorida species are arranged into the families Siphonophoridae and Siphonorhinidae, which are distinguished principally by their antennae and head forms (Shelley 1996; Moritz and Parra-Gómez 2023; Wesener 2023). Both families are known from Myanmar amber inclusions and are relatively common, representing 14% of the known millipede inclusions (Wesener and Moritz 2018). A species of the Siphonophoridae has been described in great detail from Myanmar amber (Jiang et al. 2019), showing significant differences from extant representatives (Su et al. 2021). Two species of Siphonophorida were recently described and assigned to the family Siphonorhinidae (Su et al. 2024), an assignment which seems to be erroneous at both the family and genus level.

However, Siphonorhinidae fossils might help to explain the unusual biogeography of the extant members of the family, which occur in California, Chile, South Africa, Madagascar, and Southeast Asia, and span from northern India to the Island of Flores in Indonesia (Moritz and Parra-Gómez 2023; Anilkumar et al. 2024). The Siphonorhinidae family currently comprises six genera and 16 extant species (Fig. 1), with recently described new genera and species from India, Madagascar, South America and North America (Marek et al. 2023; Moritz and Parra-Gómez 2023; Wesener 2023; Anilkumar et al. 2024).

Here, we describe the first unambiguous fossil member of the family Siphonorhinidae from Myanmar amber. The incorporation of synchrotron and μ-CT data provides a detailed morphological reconstruction of the species, which resembles the descriptions of the extant forms.

Methods

Abbreviations

3D Three-Dimensional
CT Computed Tomography
UV Ultra Violet

Provenance, measurements and preparation

The specimen is included in a small piece of amber (round, 10.02 mm × 12.25 mm × 2.42 mm, see taphonomic description below for more details). The amber piece is from the Hukawng Valley of northern Myanmar

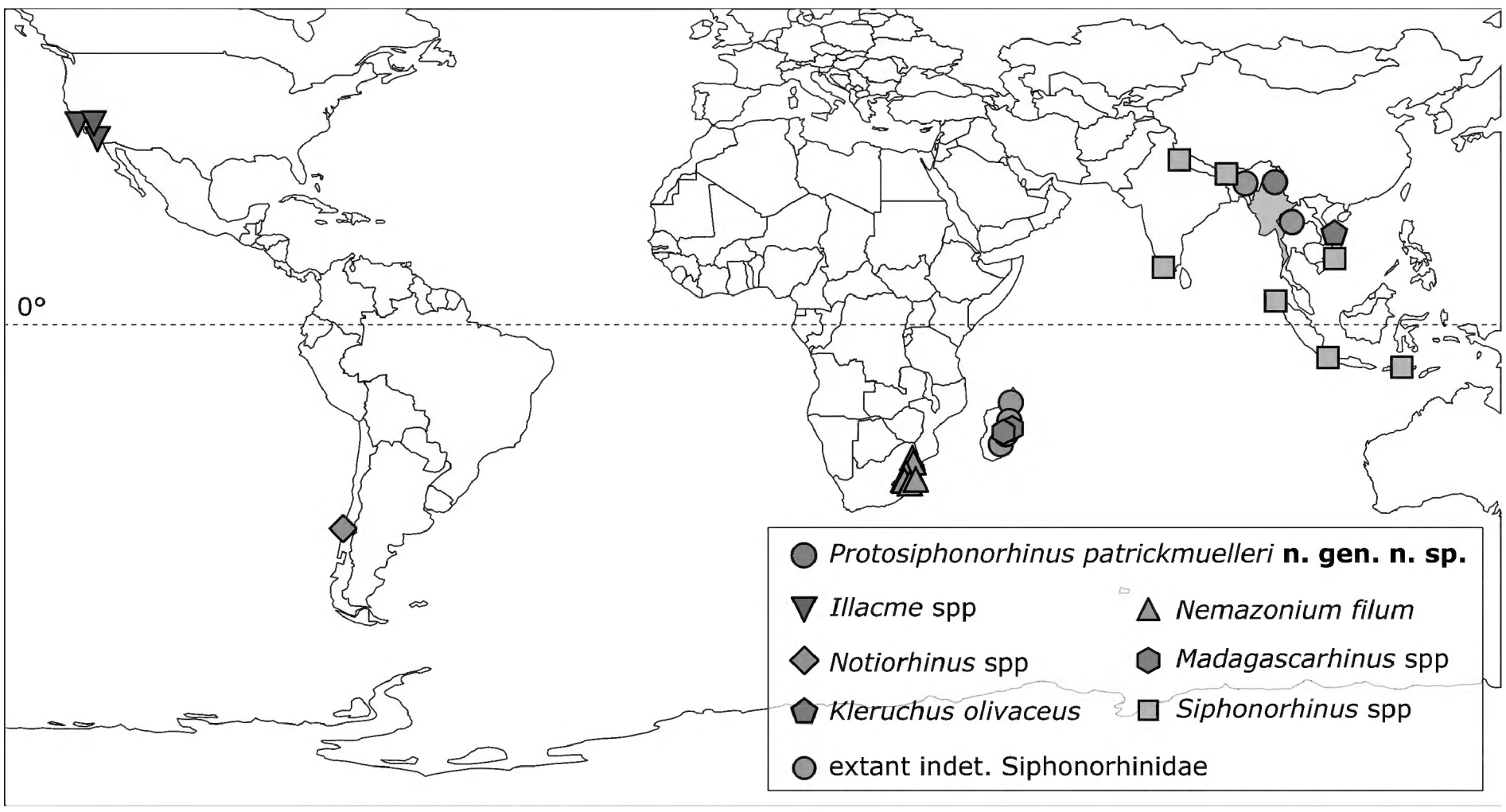

Figure 1. Distribution map of the Siphonorhinidae family. The amber piece containing *Protosiphonorhinus patrickmuelleri* is from the Hukawng Valley of northern Myanmar (Burma) (26°15′ N, 096°34′ E), corresponding to the red star.

(Burma) (26°15′N, 096°34′E) (Fig. 1). The Myanmar amber has been dated from the Upper Cretaceous, near the Albian/ Cenomanian boundary (98 ± 0.63 Ma, Shi et al. 2012) and is very rich in arthropod fossils (Ross 2019; 2022). The specimen was legally collected before February 2021 and sold in June 2016. It was loaned for study in May 2017 and later donated from the vast amber collection of Patrick Müller (Käshofen, Germany, BuB1991). Authenticity of the amber was tested using UV light, under which Myanmar amber is known to fluoresce blue. As with many amber pieces, a "window" has been polished on the surface to allow a better view of the inclusion. Measurements of the amber were taken with a digital caliper. The specimen was measured utilizing the 3D reconstruction obtained from the CT scan. Measurements were taken using ImageJ (version Java 1.8.0). Syninclusions present in the amber piece are an insect leg, a mite, and vegetal fragments (Fig. 2A, B). The piece of amber is housed currently in the collections of the Koenig Museum, in Bonn, Germany (ZFMK MYR13870).

Photographs and observations

Pictures of the specimen were taken using a Canon EOS 7D camera mounted on a P-51 Cam-Lift (Dun Inc.). The image stacks were evaluated in Adobe Lightroom (version 5.6) and stacked with Helicon Focus (version 8.2.2).

The specimen was examined using a Zeiss SteREO Discovery.V12 stereomicroscope and an Olympus BX51 light microscope.

µ-CT and three-dimensional visualization

CT data were obtained using a Bruker SKYSCAN 1272 with the following settings: source voltage: 43 kV, source current: 200 µA, 360° rotation, rotation steps: 0.165°, exposure time: 900 ms, frame averaging: 5, random movement: 15, and pixel size: 1.100686 µm. The projections were reconstructed with NRecon. Amira (version 6.5.0) was used to crop the scan and to virtually remove dirt and air bubbles via the arithmetic function. Volume renders of the reconstruction were created using VG Studio version 3.3.4 (64-bit) employing the module Phong, as well as Drishti version 2.6.3 (Limaye 2012). All images were edited, and scale bars were added using Adobe Photoshop (version 24.4.1).

Synchrotone CT

The specimen BuB1991 was measured at DESY (Deutsches Elektronen-Synchrotron – DESY, Hamburg, Germany) storage ring PETRA III, at Beamline P05 (Haibel et al. 2010; Greving et al. 2014; Wilde et al. 2016), which is operated by Hereon (Geesthacht, Germany), during beamtime 11012373 in October 2021. Measurements were performed with an energy of 18 keV, a sample-detector distance of 75 mm, an effective pixel size of 0.458047 µm, and 3501 projections using a 20 MP CMOS camera system (Lytaev et al. 2014). Reconstruction was performed in Matlab (MathWorks) and Astra Toolbox (Palenstijn et al. 2011; van Aarle et al. 2015, 2016) in a custom reconstruction pipeline (Moosmann et al. 2014) using filtered back-projection. Data were binned three times, resulting in a pixel size of 1.37414 µm. The resulting image stack was cropped, rotated, and contrast-adjusted in Fiji ImageJ version 1.53c (Schindelin et al. 2012). Volume rendering of the SR-µCT data was done in Drishti version 3.0 (Limaye 2012).

Data availability

Supplementary data, the synchrotone and micro-CT scans underlying this article, can be found at Moritz et al. 2025 (https://doi.org/10.5281/zenodo.14969051).

Results

Class Diplopoda de Blainville, 1844 in Gervais, 1844
Subclass Helminthomorpha Pocock, 1887

Order Siphonophorida Newport, 1844

Remarks. For a diagnosis of the order, see Sierwald et al. (2003) and Enghoff et al. (2015).

Family Siphonorhinidae Cook, 1895

Type genus. *Siphonorhinus* Pocock, 1894. Eight species.

Placement of the new species in the family. The new species of the new genus is placed in the family Siphonorhinidae based on the following characters: the head being pear-shaped, neither elongate nor with a long beak (like in members of the Siphonophoridae) (Figs 2C, 3A– C); antennomere 2 slender, longer than wide (usually wider than long in Siphonophoridae); antennae elbowed between antennomeres 3 and 4 (antennae straight in Siphonophoridae); anterior margin of collum straight (emarginate in Siphonophoridae) (Figs 2C, 3B, C).

† *Protosiphonorhinus* gen. nov.
https://zoobank.org/7DF0C408-8E63-4EA5-84C9-E6B96A20A89E

Type species. *† Protosiphonorhinus patrickmuelleri* sp. nov.

Derivation of name. From Greek "*prôtos*" (first, earliest) + pre-existing generic name *Siphonorhinus*, meaning ancestor of the extant genus. Gender masculine.

Diagnosis. *Protosiphonorhinus* gen. nov. species are small (7 mm), short (<40 tergites) (Figs 2A, B, 3A), setose siphonorhinids with neither paranota nor spines surrounding the ozopore (Figs 2F, 3G). Metazonites smooth except for setation; ozopores located in posterior-most lateral corners of tergite, without peculiarities (Figs 2C, 3G).

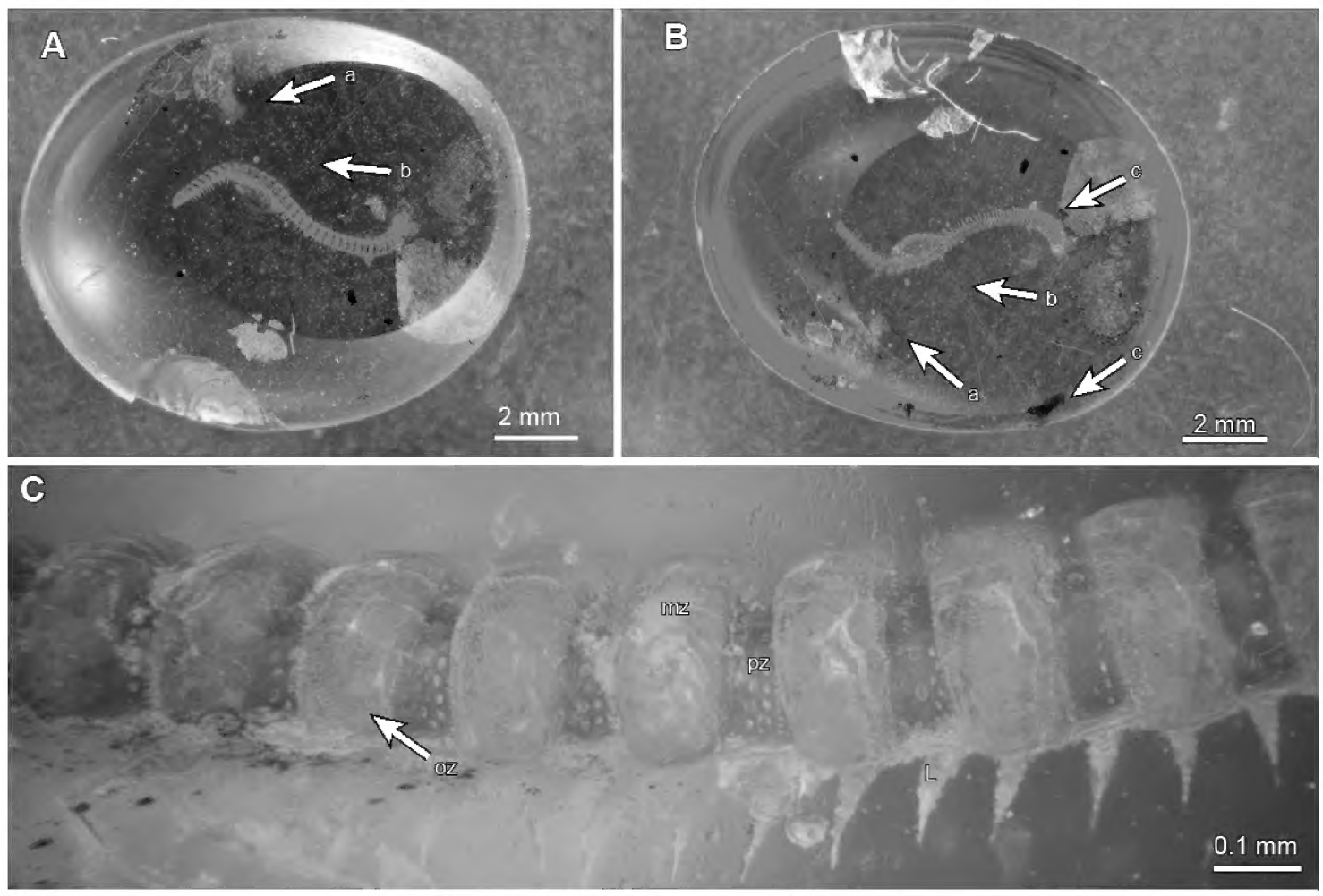

Figure 2. *Protosiphonorhinus patrickmuelleri* gen. et sp. nov., holotype (ZFMK MYR13870) in Myanmar Amber (BuB1991), photography. **A**. Amber inclusion, *Protosiphonorhinus patrickmuelleri* gen. et sp. nov., dorsal view, a = insect leg, b = mite; **B**. Amber inclusion, *Protosiphonorhinus patrickmuelleri* gen. et sp. nov., ventral view, a = insect leg, b = mite, c = wood fragment; **C**. Mid-body, lateral view; **D**. Head and first segments, lateral view; **E**. Left antennae and first segments, lateral view; **F**. Left antennae, lateral view. **Abbreviations**: I–VII = antennomeres, Co = collum, d = apical disc, ga = anterior gonopods, gp = posterior gonopods, L = leg, la = labrum, mz = metazonite, oz = ozopore, p = sensory pit, pz = prozonite, T2–T7 = tergites.

First leg in males is unmodified; coxa not fused to sternite /stigmatic plate (Fig. 3E). Head pear-shaped (Figs 2D, 3A–C). Anterior gonopod consists of 7 podomeres with a rectangular posterior process on podomere 5 (Fig. 4A–E). Antenna features an only weakly elongated but slender antennomere 2 and a massively enlarged and swollen (resembling a citron) antennomere 6, with deep pits present laterally on antennomeres 5 and 6 (Figs 2D–F, 3A–C).

Protosiphonorhinus gen. nov. differs with 7 podomeres in the anterior gonopod (Figs 4A–E)– as present in *Illacme* (see Marek et al. 2016, 2023), *Notiorhinus* (see Moritz and Parra-Gómez 2023), and *Madagascarhinus* (see Wesener 2023) from *Kleruchus* (see Attems 1938), *Nematozonium* (see Shelley and Hoffman 2004), and *Siphonorhinus* (see Anilkumar et al. 2024) with 6 podomeres in the anterior gonopods.

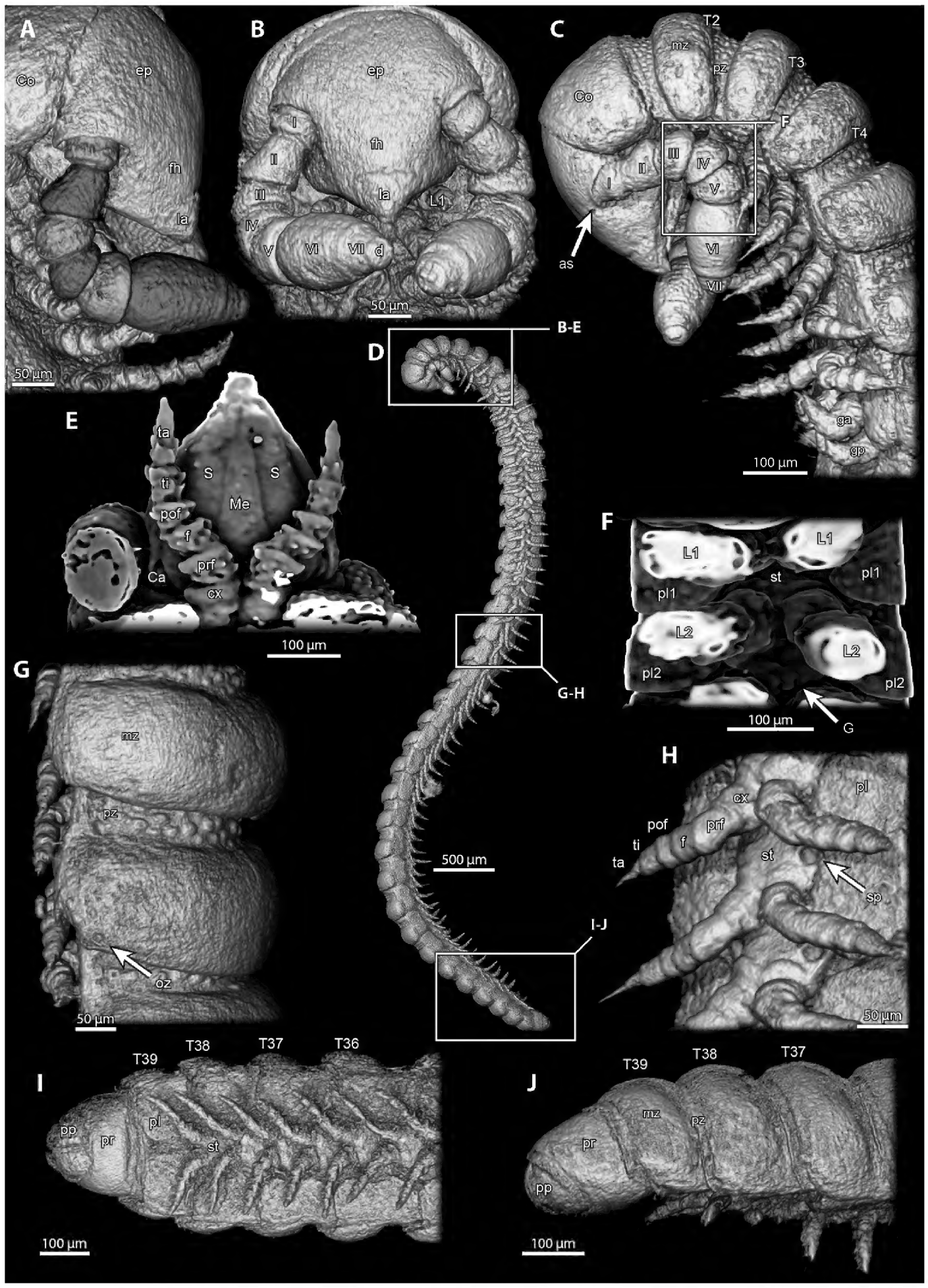

Figure 3. *Protosiphonorhinus patrickmuelleri* gen. et sp. nov., holotype (ZFMK MYR13870) in Myanmar Amber (BuB1991), reconstructions. **A**. Entire body; **B**. Head, lateral view; **C**. Head, ventral view; **D**. Head and first segments, lateral view; **E**. Gnathochilarium and first leg pair, ventral view; **F**. Gonopores, ventral view; **G**. Mid- body legs, anterior- lateral view; **H**. Mid- body, ventral view; **I**. Posterior body-rings and telson, ventral view; **J.** Posterior body-rings and telson, lateral view. **Abbreviations**: I–VII = antennomeres, as = antennal socket; Ca = cardines of mandible; Co = collum, cx = coxa, d = apical disc, ep = epicranium, f = femur, fh = forehead, ga = anterior gonopods, gp = posterior gonopods, G = gonopores, Me = mentum, L1 = first leg pair, L2 = second leg pair, la = labrum, mz = metazonite, oz = ozopore, pl = pleurite, pof = postfemur, pp = paraproct (anal valve), pr = preanal ring, prf = prefemur, pz = prozonite, S = stipe, st = sternite, sp = spiracle, T2–T39 = tergites, ta = tarsus, ti = tibia.

Protosiphonorhinus gen. nov. differs from all known genera in the small number of segments present in mature specimens (<40), with species of *Madagascarhinus* Wesener, 2023, and *Siphonorhinus* being closest (starting at 60). *Protosiphonorhinus* gen. nov. shares only with the Asian representatives of the family – the monotypic *Kleruchus* Attems, 1938, and *Siphonorhinus* – the presence of pits on antennomeres 5 and 6 (Fig. 2D, E), which are absent in all other Siphonorhinidae genera. *Protosiphonorhinus* gen. nov. differs from both extant Asian genera in the absence of paranota (Fig. 2C) (present in both *Siphonorhinus* and *Kleruchus*), as well as the presence of a lemon-shaped antennomere 6 which reaches its greatest width medially (Figs 2D, 3A–C) (antennomere 6 cylindrical in *Kleruchus*, vastly swollen reaching its greatest width more apically in *Siphonorhinus*).

† *Protosiphonorhinus patrickmuelleri* sp. nov.

https://zoobank.org/A6946237-D3C7-4A71-BB3B-2EDE200D80CE

Material examined. 1 ♂ holotype, ZFMK MYR13870, preserved in amber from the Burmese Kachin region, Hukawng valley. Exported before 2017, donated from the vast amber collection of Patrick Müller (Käshofen, Germany, BuB1991).

Derivation of name. Adjective, after the collector and donator.

Diagnosis. As the genus is monotypic, the genus diagnosis is the same as the species diagnosis.

In case additional species are discovered in Myanmar amber in the future, the surface of the prozonites and metazonites, the location of the ozopores starting at tergite 6 (Figs 2C, 3G), and the pear-shape of the head necessitate examination (Figs 2D, 3A–C). The gonopods of *Protosiphonorhinus patrickmuelleri* gen. et sp. nov. are peculiar, with both anterior and posterior gonopods consisting of seven podomeres (Fig. 4A–E). Apical-most podomere of posterior gonopod, often carrying species-specific characters in extant species of the family, is unfortunately only partly preserved (Fig. 4B).

Taphonomic notes. The holotype is preserved in a piece of amber whose shape is round and which measures 10.02 mm in width, 12.25 mm in length, and 2.42 mm in thickness. The color is light orange, with good transparency. Syninclusions present in our amber piece are an insect leg, a mite, and vegetal fragments (Fig. 2A, B).

Description. ***Body*:** elongated (Figs 2A, B, 3D), 18 times longer than wide, half-cylindrical. Measuring around 6.9 mm in length, with 38+1 body rings plus telson (Fig. 3D). Each tergite approximately 0.38 mm wide. Setation of the head not visible (Fig. 2C). Color between dark orange and yellow, in light-orange colored amber (Figs 2A, B).

***Head*:** pear-shaped, tapering anteriorly. Longer than wide, length of 0.3 mm (Fig. 3A, B). Epicranium and forehead smoothly rounded, without delimitation. Epicranium partially arching above the antennal socket. Labrum triangular, visibly delimited in the anterior part of the head, encompassing approximately one-fifth of the head length, with a lighter color and slightly extending ventrally (Figs 2D, 3A, B). Genae (area laterally below antennae) almost straight, extending below the lateral extension of the collum. Head below antennae (at genae) ca. three-quarters of the width of the epicranium above antennae. Ventral margin of head capsule apically slightly concave (Fig. 3B, C). No eyes (Fig. 3A). No organ of Tömösváry visible.

Gnathochilarium triangular, tightly appressed to the head capsule, with at least five well-distinguishable plates (proximal part obscured by legs) (Fig. 3E): two lateral stipites, two apical mesal lamellae linguales, and a central mentum. The apical-most part (lamellae linguales) is difficult to observe. Mandibular cardo visible in ventral view, mandibular stipes and gnathal lobe internalized, not visible externally (Fig. 3E).

Antennae laterally inserted on the posterior part of the head, in antennal socket, which opens fronto-lateral (ca. 45° angle) (Fig. 3C). Antennae consisting of seven antennomeres plus an apical disc, protruding if stretched out up to the posterior margin of segment 4. Elbowed between antennomeres 3 and 4 (Figs 2D, 3A–C). Antennomere 1 cylindrical, wider but shorter than antennomere 2. Antennomere 2 slender, almost as long as antennomeres 3 and 4 combined. Antennomeres 3 and 4 of equal width and length. Antennomere 5 slightly wider and longer. Antennomere 6 massive, swollen, with a lemon shape reaching its widest point at ca. one-third of its length, tapering towards antennomere 7, wider and as long as combined antennomeres 3, 4, and 5. Antennomere 7 very small, as large as one-fifth of antennomere 6 and terminated by an apical disc (Figs 2D, 3A–C). Relative lengths of antennomeres: 7 < 1 < 3 = 4 < 2 < 5 < 6. Each antennomere is covered by numerous small setae, the length of setae ca. 0.05 times the diameter of the antennomere (Fig. 2C). Sensilla basiconica not visible, but two sensory pits are situated latero-apically on antennomeres 5 and 6 (Fig. 2E, F). The pit on antennomere 6 is significantly large, as large as one-quarter to one-third of the antennomere length (Fig. 2F, E). The terminal disk with the usual four large apical cones, smaller sensillae not observable (Fig. 3B).

***Body rings*:** Anterior margin of collum straight. Collum at least twice as long but not extending as far ventrally as following tergites, and only slightly overlapping head (Fig. 3B, C). Each mid-body ring composed of one tergite, two pleurites, and two sternites, well differentiated and not fused. Tergites without paranota or paraterga. Tergites divided into prozonite and metazonite (Figs 2C, 3G). Metazonite wider and almost twice as long as prozonite, strongly arched, colored in a light orange color. Metazonite surface smooth, dirty, covered with some small setae, more concentrated at the posterior margin (Fig. 2C). Prozonites covered with longitudinally 16–19 and latitudinally three or four round protuberances, lacking setae, and colored in a darker orange (Figs 2C, 3G). Posterior margin of metazonite (limbus) with rectangular projections whose posterior margin is toothed (Fig. 2C). Tergites decreasing in width in the posterior part of the body (Fig. 3D). Starting at the fifth tergite, ozopores are laterally posteriorly situated on metazonite, close to the posterior margin (Figs 2C, 3G). Ozopores not marked and not surrounded by visible setae or sensillae, difficult to distinguish on some tergites. Ozopore at least on some tergites slightly projecting posteriorly on the posterior tergite margin (Fig. 3G).

Pleurite surfaces are covered with around eight rows of round protuberances, similar to those of prozonite (Fig. 3H). Legs attached to the sternite portions of body rings (Figs 3G, H). Large paired spiracles present on the sternites, posteriorly to legs (Fig. 3F). Sternites without a projection between the coxae, surface irregular, with some protuberances not well discernible (Fig. 3H). One apodous ring and telson at the posterior end of the body, covered by numerous small setae (Fig. 3I, J). Anal valves of telson well-developed, also covered by protuberances (Fig. 3I, J). Subanal scale (epiproct) small.

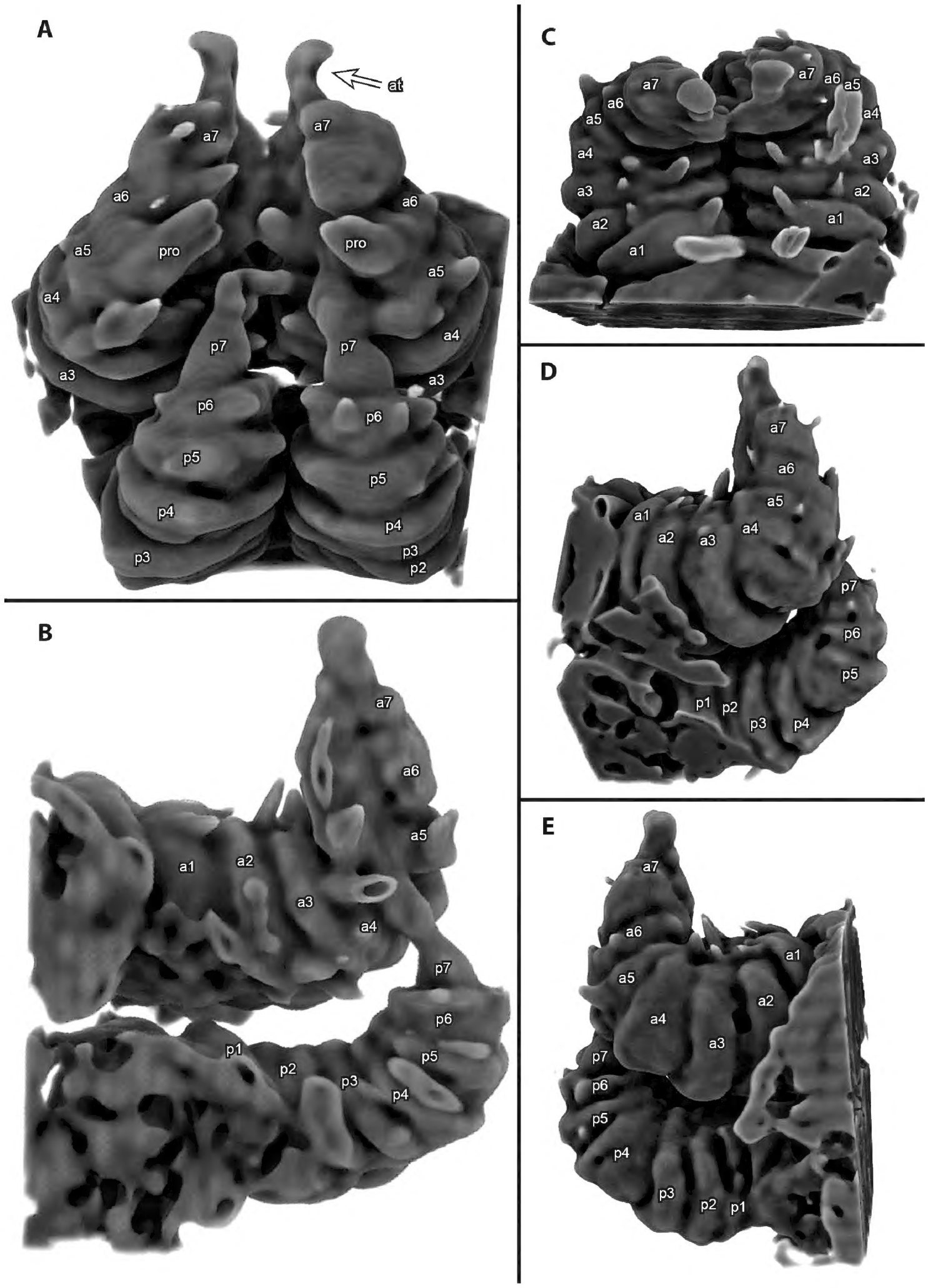

Figure 4. *Protosiphonorhinus patrickmuelleri* gen. et sp. nov., holotype (ZFMK MYR13870) in Myanmar Amber (BuB1991), Synchrotone micro-CT volume rendering. **A**. Gonopods, ventral view; **B**. Right gonopod, mesal view; **C**. Anterior gonopod, posterior view; **D**. Gonopods, lateral view; **E**. Gonopods, lateral view. **Abbreviations**: a1–a7 = podomeres of the anterior gonopod, at = apical termination, p1–p7 = podomeres of the posterior gonopods, pro = projection.

***Legs*:** Six podomeres, coxa, prefemur, femur, postfemur, tibia, and tarsus, terminated by a claw (Fig. 3E, H). First legs shorter than the head and comparing to mid-body leg (Fig. 3E). Elongated tarsus with no visible claw. First prefemur, femur, and tibia of similar length. Prefemur and femur wider than longer. Tibia longer than wider. Shorter postfemur, wider than long. First sternite with a smooth surface. Second leg pair with wider than longer prefemur and femur, smaller postfemur, and an elongated tibia. Tarsus elongated and terminated by an apical claw. Lobe posteriorly on the coxa of the second leg pair inferred to be male gonopores (Fig. 3F). Midbody legs with elongated tarsus and claw (Fig. 3H). Tarsus slenderer, less than half as wide as other podomeres, apically tapering. Triangular and wide coxa. Relative size of podomeres in midbody legs: postfemur < tibia < prefemur < femur < coxa < tarsus (Fig. 3H). Elongated apical claw with no visible apical spine/accessory claw. Long spines present on each podomere. Tarsus shorter in anterior and posterior legs than on midbody legs. General mid-body leg length equal to half the body width

of the ventral side (Fig. 3H). Posterior legs comparatively shorter, measuring only one-third of the body width (Fig. 3I). Five anterior-most legs curved and ventrally oriented (Fig. 3C). Other legs extended and laterally oriented (Fig. 3C, D). Coxal sacs visible and weakly everted on some legs. Leg pairs 9 and 10 modified into gonopods (Fig. 3C).

***Gonopods*:** Two pairs of gonopods situated posteriorly to the eighth leg pair and curved anteriorly (Fig. 3C). Anterior pair (leg 8) consisting of seven podomeres without fusion (Fig. 4A–E). Podomeres 1 to 6 cylindrical, each carrying setae, especially well developed on anterior side (massive, almost spine-like appearance of these setae is probably a preservation artefact). Podomere 4 at posterior margin apparently with wide, well-rounded process projecting as far as apical end of podomere 5. Podomere 7 elongated with apical tip curved laterally (Fig. 4A). Podomeres 5–7 ventrally projecting and apically curved, forming protection sheath for posterior gonopods (Fig. 4A, B).

Posterior gonopod (leg 9) consisting of seven podomeres, without fusion and with podomeres 1 to 6 cylindrical (Fig. 4A, B, D, E). Ultimate podomere elongated and expanded into filamentous process, resting in mesal sheath formed by apical podomeres of anterior gonopod. Apex of ultimate podomere not visible. Process protruding at least as far as the sixth anterior podomere (Fig. 4B). Posterior gonopod with short setae.

Discussion

Preservation artifacts or unusual characters

Two characters in *Protosiphonorhinus patrickmuelleri* gen. et sp. nov. are rather unusual and have not been observed in the few extant relatives of the family: the 'step' or fold towards the labrum on the head (Figs 2D, 3A–C) and the unusually large antennal pits on antennomeres 5 and 6 (Fig. 2E, F). Both characters are visible in the µ-CT scan (Fig. 3A–C), the synchrotron CT-scan, and optically under the microscope (Fig. 2E, F). A similar fold at the transition of the labrum to the forehead can be found in a recent description of the extant genus *Illacme* (see Marek et al. 2016, fig. 2). The cuticle of the labrum is quite thin, suggesting a possible shrinking artifact. Whether or not these characters are artifacts created during the complex preservation process in amber needs to be further investigated once more specimens of *Protosiphonorhinus patrickmuelleri* gen. et sp. nov. become available.

Diversity of the family Siphonorhinidae in the Cretaceous

Members of the Siphonorhinidae are not rare in Myanmar amber, with at least 12 specimens (two males, ten females) reported as of 2018 (Wesener and Moritz 2018) in addition to the specimen described here, which Wesener and Moritz (2018) listed as an undetermined Siphonophorida with the identifier BuB1991. Since 2018, an additional 11 specimens (three male, eight female) have been sent to one of us (TW) for determination (unpublished), leading to a total of 5 male and 18 female Siphonorhinidae. All five available males clearly do not belong to *Protosiphonorhinus* gen. nov. as they have differently shaped antennae and/or strongly developed paranota, but a description of those specimens is beyond the scope of this article. Although some colobognathan Platydesmida appear to have undergone little change since the Cretaceous, closely resembling the morphology of extant genera (Moritz and Wesener 2019), the Cretaceous Siphonophorida have been shown to differ quite drastically from extant representatives, e.g., with a divided gnathochilarium (Su et al. 2021). In a similar manner, the Siphonorhinidae described here differ in their character combination from extant genera.

Remarks on two recently described fossil Siphonophorida assigned to the wrong family and/or genus

During the first submission process of this publication, Su et al. (2024) described two representatives of the genus *Siphonorhinus* within the family Siphonorhinidae: *Siphonorhinus globosus* Su, Cai & Huang, 2024 and *Siphonorhinus peculiaris* Su, Cai & Huang, 2024 (Su et al. 2024). However, the specimens described as *S. globosus* are clearly representatives of the family Siphonophoridae as evident from 1) the short but pronounced beak (Su et al. 2024: 71; figs 2B, 5D) and 2) the straight (not elbowed!) antennae, consisting of stout uniform antennomeres (Su et al. 2024: figs 1D, 4C, 5C, 6E). 1) The globose head shows an abrupt transition into a short beak, which is free from setae. Such short beaks are known from representatives of the extant South American genus *Columbianum* Verhoeff, 1941 (see Read and Enghoff 2018) and some representatives of the genus *Siphonophora*, such as *S. zelandica* Chamberlin, 1920 and *S. feae* Pocock, 1893, within the family Siphonophoridae. 2) While the antennae of Siphonorhinidae are typically elbowed and have an elongated second antennomere (see Marek et al. 2023 for *Illacme*; Attems, 1938 for *Kleruchus*, Anilkumar et al. 2024 for *Siphonorhinus*; Wesener 2023 for *Madagascarhinus*; Shelley and Hoffman 2004 for *Nematozonium*; Moritz and Parra-Gómez 2023 for *Notiorhinus*), the specimens described by Su et al. (2024) clearly have straight antennae with stout antennomeres of uniform size. Therefore, we suggest the placement of the species in the genus *Siphonophora* Brandt, 1837 as *Siphonophora globosa* comb. nov.

The generic placement of *Siphonorhinus peculiaris* is questionable at best, as the characters Su et al. (2024: 87) argue to support this "confident" placement are not specific for the genus and are generally found in the family Siphonorhinidae, or they cannot be observed in *S. peculiaris*. The head is small, not extending into a rostrum, and lack ommatidia (like in all Siphonophorida), and the antenna is swollen and elbowed in all Siphonorhinidae (e.g., Enghoff et al. 2015; Moritz and Parra-Gómez 2023). Furthermore, the sensilla basiconica of *S. peculiaris* are

arranged in rows (Su et al. 2024: 80, fig. 12D-F), while in representatives of *Siphonorhinus* these are sunken into sensory pits (e.g., Attems 1930, 1938; Anilkumar et al. 2024), as is also the case in *Kleruchus*. Therefore, the specimens might represent an extinct, highly derived lineage or a stem lineage within Siphonorhinidae, but they do not represent a species of the genus *Siphonorhinus*.

Contrary to the arguments made by the authors, their fossils do not allow any conclusion about the origin of the genus *Siphonorhinus*, nor provide support to the hypothesis by Su et al. (2024) of "extreme bradytely within the Siphonorhinidae from the mid-Cretaceous to the present day."

Conclusions

The first fossil of the extant millipede family Siphonorhinidae is described from Myanmar amber. 3D-reconstructions based on synchrotron and µ-CT, as well as light microscopy, enable the visualization of several important morphological structures, including the gonopods, facilitating a precise description and determination of the specimen. While our Myanmar amber fossil shares some characteristics with the extant genus *Siphonorhinus*, it exhibits clear differences in numerous traits, warranting its placement in the new genus, *Protosiphonorhinus* gen. nov.. Our findings refute the hypothesis of bradytely within the Siphonorhinidae from the mid-Cretaceous to the present day.

Acknowledgements

We sincerely thank Mr. Patrick Müller, owner of a large collection of arthropods and other objects in Myanmar Amber, who arranged the transfer of the type specimens to the collections of the ZFMK and donated the valuable holotype of *Protosiphonorhinus patrickmuelleri*. Synchrotron-based-CT data was obtained at DESY, PETRA III, Beamline P05 which is operated by Hereon (Geesthacht, Germany) during beamtime 11012373. We thank Jörg Hammel for assistance and support during the Beamtime. Thanks also to Jonathan Vogel for the specimen pictures. Many thanks to Luce Gay for her technical assistance and intellectual support. Their contributions have been instrumental in the success of this project, and we are grateful for their valuable help.

We thank the three anonymous reviewers and the editor for their comments which greatly improved the quality of the here presented work.

Most of the reconstruction data was created by Ms. Solène Bourdas during a stay at the LIB which was part of a module conducted in the international Master program Organismic Biology, Evolutionary Biology and Paleobiology (OEP-Biology) at the Rheinische Friedrich-Wilhelms University of Bonn, Germany.

This research did not receive any specific grant from funding agencies in the public, commercial, or not-for-profit sectors.

References

Anilkumar PA, Wesener T, Moritz L (2024) Integrative description of a new species of the millipede genus *Siphonorhinus* Pocock, 1894 and first record of the family Siphonophoridae from India (Diplopoda, Colobognatha, Siphonophorida). Integrative Systematics 7(2): 1–21. https://doi.org/10.18476/2024.533955

Attems C (1930) Myriopoden der Kleinen Sunda-Inseln, gesammelt von der Expedition Dr. Rensch. Mitteilungen aus dem Zoologischen Museum in Berlin 16(1): 117–184. https://doi.org/10.1002/mmnz.19300160103

Attems C (1938) Die von Dr. C. Dawydoff in Französisch Indochina gesammelten Myriopoden. Mémoires du Muséum national d'Histoire naturelle, N.S., 6(2): 187–353.

Crawford CS (1992) Millipedes as model detritivores. Berichte des Naturwissenschaftlich-Medizinischen Verein Innsbruck 10: 277–288.

Cruickshank RD, Ko K (2003) Geology of an amber locality in the Hukawng Valley, Northern Myanmar. Journal of Asian Earth Sciences 21(5): 441–455. https://doi.org/10.1016/S1367-9120(02)00044-5

Curry JP (1994) Grassland Invertebrates. Chapman and Hall, London, UK, 437 pp.

Enghoff H, Golovatch S, Short M, Stoev P, Wesener T (2015) Diplopoda—taxonomic overview. Treatise on Zoology-Anatomy, Taxonomy, Biology. The Myriapoda 2: 363–453. https://doi.org/10.1163/9789004188273_017

Friis EM, Pedersen KR, Crane PR (2006) Cretaceous angiosperm flowers: innovation and evolution in plant reproduction. Palaeogeography, Palaeoclimatology, Palaeoecology 232(2–4): 251–293. https://doi.org/10.1016/j.palaeo.2005.07.006

Greving JP, Wermer MJ, Brown RD, Morita A, Juvela S, Yonekura M, Algra A (2014) Development of the PHASES score for prediction of risk of rupture of intracranial aneurysms: a pooled analysis of six prospective cohort studies. The Lancet Neurology 13(1): 59–66. https://doi.org/10.1016/S1474-4422(13)70263-1

Grimaldi D (1999) The co-radiations of pollinating insects and angiosperms in the Cretaceous. Annals of the Missouri Botanical Garden, 373–406. https://doi.org/10.2307/2666181

Grimaldi DA, Engel MS, Nascimbene PC (2002) Fossiliferous Cretaceous amber from Myanmar (Burma): its rediscovery, biotic diversity, and paleontological significance. American Museum Novitates 3361: 1–71. https://doi.org/10.1206/0003-0082(2002)361%3C0001:FCAFMB%3E2.0.CO;2

Haibel A, Manke I, Melzer A, Banhart J (2010) In situ microtomographic monitoring of discharging processes in alkaline cells. Journal of the Electrochemical Society 157(4): A387. https://doi.org/10.1149/1.3294566

Hoffman RL (1980) Classification of the Diplopoda. Museum d'Histoire Naturelle, 237 pp.

Jeekel CAW (2001) A bibliographic catalogue of the Siphonophorida (Diplopoda). Myriapod Memoranda 3: 44–71.

Jiang X, Shear WA, Hennen DA, Chen H, Xie Z (2019) One hundred million years of stasis: *Siphonophora hui* sp. nov., the first Mesozoic sucking millipede (Diplopoda: Siphonophorida) from mid-Cretaceous Burmese amber. Cretaceous Research 97: 34–39. https://doi.org/10.1016/j.cretres.2019.01.011

Limaye A (2012) Drishti: a volume exploration and presentation tool. In Developments in X-ray Tomography VIII 8506: 191–199. https://doi.org/10.1117/12.935640

Marek PE, Shear WA, Bond JE (2012) A redescription of the leggiest animal, the millipede *Illacme plenipes*, with notes on its natural history and biogeography (Diplopoda, Siphonophorida, Siphonorhinidae). ZooKeys 241: 77. https://doi.org/10.3897/zookeys.241.3831

Marek PE, Krejca JK, Shear WA (2016) A new species of Illacme Cook & Loomis, 1928 from Sequoia National Park, California, with a world catalog of the Siphonorhinidae (Diplopoda, Siphonophorida). ZooKeys (626): 1.

Marek PE, Hall CL, Lee C, Bailey J, Berger MC, Kasson MT, Shear W (2023) A new species of *Illacme* from southern California (Siphonophorida, Siphonorhinidae). ZooKeys 1167: 265. https://doi.org/10.3897/zookeys.1167.102537

Moosmann J, Ershov A, Weinhardt V, Baumbach T, Prasad MS, LaBonne C, Hofmann R (2014) Time-lapse X-ray phase-contrast microtomography for in vivo imaging and analysis of morphogenesis. Nature Protocols 9(2): 294–304. https://doi.org/10.1038/nprot.2014.033

Moritz L, Wipfler B, Wesener T (2025) Micro-CT data of *Protosiphonorhinus patrickmuelleri* (ZFMK MYR13870/BuB1991). Zenodo. https://doi.org/10.5281/zenodo.14969051

Moritz L, Parra-Gómez A (2023) *Notorhinus floresi* sp. nov. gen. nov.: The first records of Siphonophorida in Chile and Siphonorhinidae in South America (Colobognatha). Arthropod Systematics & Phylogeny 81: 565–579. https://doi.org/10.3897/asp.81.e100520

Moritz L, Wesener T (2018) *Symphylella patrickmuelleri* sp. nov. (Myriapoda: Symphyla): The oldest known Symphyla and first fossil record of Scolopendrellidae from Cretaceous Burmese amber. Cretaceous Research 84: 258–263. https://doi.org/10.1016/j.cretres.2017.11.018

Moritz L, Wesener T (2019) The first known fossils of the Platydesmida—an extant American genus in Cretaceous amber from Myanmar (Diplopoda: Platydesmida: Andrognathidae). Organisms, Diversity & Evolution 19: 423–433. https://doi.org/10.1007/s13127-019-00408-0

Moritz L, Wesener T (2021) Electrocambalidae fam. nov., a new family of Cambalidea from Cretaceous Burmese amber (Diplopoda, Spirostreptida). European Journal of Taxonomy 755: 22–46. https://doi.org/10.5852/ejt.2021.755.1397

Limaye A (2012) Drishti: a volume exploration and presentation tool. In Developments in X-ray Tomography VIII, 8506: 191–199. https://doi.org/10.1117/12.935640

Lytaev P, Hipp A, Lottermoser L, Herzen J, Greving I, Khokhriakov I, Beckmann F (2014) Characterization of the CCD and CMOS cameras for grating-based phase-contrast tomography. In Developments in X-Ray Tomography IX 9212: 318–327. https://doi.org/10.1117/12.2061389

Palenstijn WJ, Batenburg KJ, Sijbers J (2011) Performance improvements for iterative electron tomography reconstruction using graphics processing units (GPUs). Journal of Structural Biology 176(2): 250–253. https://doi.org/10.1016/j.jsb.2011.07.017

Read HJ, Enghoff H (2018) Siphonophoridae from Brazilian Amazonia Part 1–The genus *Columbianum* Verhoeff, 1941 (Diplopoda, Siphonophorida). European Journal of Taxonomy, 477 pp. https://doi.org/10.5852/ejt.2018.477

Ross AJ (2019) Burmese (Myanmar) amber checklist and bibliography 2018. Palaeoentomology 2(1): 22–84. https://doi.org/10.11646/palaeoentomology.2.1.5

Ross AJ (2022) Supplement to the Burmese (Myanmar) amber checklist and bibliography, 2021. Palaeoentomology 5(1): 027–045. https://doi.org/10.11646/palaeoentomology.5.1.4

Schaefer M (1990) The soil fauna on a beech forest on limestone: Trophic structure and energy budget. Oecologia 82: 128–136. https://doi.org/10.1007/BF00318544

Schindelin J, Arganda-Carreras I, Frise E, Kaynig V, Longair M, Pietzsch T, Cardona A (2012) Fiji: an open-source platform for biological-image analysis. Nature Methods 9(7): 676–682. https://doi.org/10.1038/nmeth.2019

Shelley RM (1996) The milliped order Siphonophorida in the United States and northern Mexico. Virginia Museum of Natural History. Myriapodologica 4: 21–33

Shelley RM, Hoffman RL (2004) A contribution on the South African millipede genus, *Nematozonium* Verhoeff, 1939 (Siphonophorida: Siphonorhinidae). African Entomology 12(2): 217–222.

Shi G, Grimaldi DA, Harlow GE, Wang J, Wang J, Yang M, Li X (2012) Age constraint on Burmese amber based on U–Pb dating of zircons. Cretaceous research, 37: 155–163. https://doi.org/10.1016/j.cretres.2012.03.014

Sierwald P, Shear WA, Shelley RM, Bond JE (2003) Millipede phylogeny revisited in the light of the enigmatic order Siphoniulida. Journal of Zoological Systematics and Evolutionary Research 41(2): 87e99. https://doi.org/10.1046/j.1439-0469.2003.00202.x

Su YT, Cai CY, Huang DY (2021) Morphological revision of *Siphonophora hui* (Myriapoda: Diplopoda: Siphonophoridae) from the mid-Cretaceous Burmese amber. Palaeoentomology 4(3): 279–288. https://doi.org/10.11646/palaeoentomology.4.3.15

Su YT, Cai CY, Huang DY (2022) A new species of Trichopolydesmidae (Myriapoda, Diplopoda, Polydesmida) from the mid-Cretaceous Burmese amber. Palaeoentomology 5(6): 606–622. https://doi.org/10.11646/palaeoentomology.5.6.10

Su YT, Cai CY, Huang DY (2024) Two new species of Siphonorhinidae (Myriapoda: Diplopoda: Siphonophorida) from mid-Cretaceous Burmese amber. Mesozoic 1(1): 70–89. https://doi.org/10.11646/mesozoic.1.1.6

Van Aarle W, Palenstijn WJ, De Beenhouwer J, Altantzis T, Bals S, Batenburg KJ, Sijbers J (2015) The ASTRA Toolbox: A platform for advanced algorithm development in electron tomography. Ultramicroscopy 157: 35–47. https://doi.org/10.1016/j.ultramic.2015.05.002

Van Aarle W, Palenstijn WJ, Cant J, Janssens E, Bleichrodt F, Dabravolski A, Sijbers J (2016) Fast and flexible X-ray tomography using the ASTRA toolbox. Optics Express 24(22): 25129–25147. https://doi.org/10.1364/OE.24.025129

Wesener T, Moritz L (2018) Checklist of the Myriapoda in Cretaceous Burmese amber and a correction of the Myriapoda identified by Zhang (2017). Check List 14(6): 1131–1140. https://doi.org/10.15560/14.6.1131

Wesener T (2023) *Madagascarhinus*, a new genus of the family Siphonorhinidae with two new species from Madagascar (Diplopoda, Siphonophorida). Zootaxa 5278(1): 163–175. https://doi.org/10.11646/zootaxa.5278.1.9

Wilde F, Ogurreck M, Greving I, Hammel JU, Beckmann F, Hipp A, Schreyer A (2016) Micro-CT at the imaging beamline P05 at PETRA III. In AIP conference Proceedings 1741(1): 030035. https://doi.org/10.1063/1.4952858

Wolters V, Ekschmitt K (1997) Gastropods, isopods, diplopods, and chilopods: neglected groups of the decomposer food web. Pages 265–306 in G. Benckiser, ed., Fauna in Soil Ecosystems. Marcel Dekker, Inc., New York, New York, USA, 42 pp.